Theoret. Appl. Mech., Vol.39, No.4, pp. 343–363, Belgrade 2012

Core structure of aligned chitin fibers within the interlamellar framework extracted from *Haliotis rufescens* nacre. Part I: implications for growth and mechanical response

Jiddu Bezares* **Robert J. Asaro†**
Vlado A. Lubarda ‡

Abstract

By means of consecutive alkaline and proteolytic treatments of the organic framework's interlamellar layers extracted from the nacre of *H. rufescens*, we have exposed a core of aligned parallel chitin fibers. Our findings both verify basic elements of the interlamellar layer structural model of Levi-Kalisman *et al.* (2001) and extend the more detailed model of Bezares *et al.* (2008, 2010). We observe *via* SEM imaging of square millimeter sized samples, which include numerous interlamellar layers and micron sized, yet nanocrystalline, $CaCO_3$ tiles whose native orientation within the shell was first documented, that the chitin fibers in all layers are aligned normal to the growth direction of the shell. Similar alignment has been suggested in the literature for two other classes of mollusks, *viz. N. rupertus* and *P. martensii* (Weiner and Traub, 1983; Wada, 1958), suggesting that this may be a more general motif. We find that in order to expose the chitin core it is necessary to first remove protein by an alkaline treatment followed by enzymatic digestion with proteinase-K. We also observe what appear to be the

*Department of Structural Engineering, University of California, San Diego, La Jolla, CA 92093, e-mail: jiddu.bezares@gmail.com

†Department of Structural Engineering, University of California, San Diego, La Jolla, CA 92093, e-mail: rasaro@ucsd.edu

‡Mechanical and Aerospace Engineering, University of California, San Diego, La Jolla, CA 92093, e-mail: vlubarda@ucsd.edu

points of traversal of the exposed chitin core by mineral bridges. The implications of these findings touch directly and most specifically upon the expected mechanical properties of organic framework layers such as stiffness and relaxation time constants, *viz.* they should be plane-orthotropic. Single interlamellar layers extracted from nacre should, by implication, also exhibit an orthotropic stiffness. These novel findings provide the structural picture required for a complete anisotropic, time dependent, constitutive description of nacre long thought to be a paradigm of structural optimization. Such a model is briefly described herein and is developed, in full, in Part II of this series.

Keywords: Biomineralization, Chitin fibers, Mollusk nacre, Mollusk organic framework.

1 Introduction

For decades the process of biomineralization has been the topic of intense research as it has provided inspiration for the design and synthesis of novel bio-mimetic materials (Sarikaya *et al.*, 1992, Baeuerlein, 2000, Ritchie, 2011). In mollusks precise control over shell growth and architecture is exerted by proteins secreted from the epithelial cells of the animal's mantle tissue (Lowenstam and Weiner, 1989; Rousseau *et al.*, 2005; Addadi and Weiner, 2006). Research has focused on the inner iridescent layer of the shell referred to as nacre due to its extraordinary mechanical properties when compared to those of its constituent materials namely calcium carbonate and protein (Srinivasan 1941; Currey, 1977; Evans *et al.*, 2001; Wang *et al.*, 2001; Bezares *et al.*, 2011). Most notably is nacre's toughness three orders of magnitude greater than that of its mineral phase (Jackson *et al.* 1988; Gao *et al.*, 2003).

The microstructure of nacre has been described as brick-wall-like as it consists of parallel alternating lamellae of $\sim$500 nm thick tiles 4-5 μm wide with interlamellar layers (il-layers) of organic material $\sim$20 nm in thickness (Fig. 1a). The imprints of tiles remain on il-layers following their extraction from nacre by demineralization (Fig. 1b). Nacre's toughness is largely due to the crack blunting and deflecting capabilities of the il-layers, making the study of their structure of principle importance.

The biochemical structure and amino acid composition of il-layers which form a 3-dimensional framework have been characterized (Gregoire, 1957, 1972; Crenshaw and Ristedt, 1976; Nudelman *et al.*, 2006; Cariolou and Morse, 1988). Il-layers consist of 75-80 wt% aspartic acid rich glycoproteins Addadi and Weiner, (1985) and chitin (Peters, 1972; Goffinet and Jeaniaux,

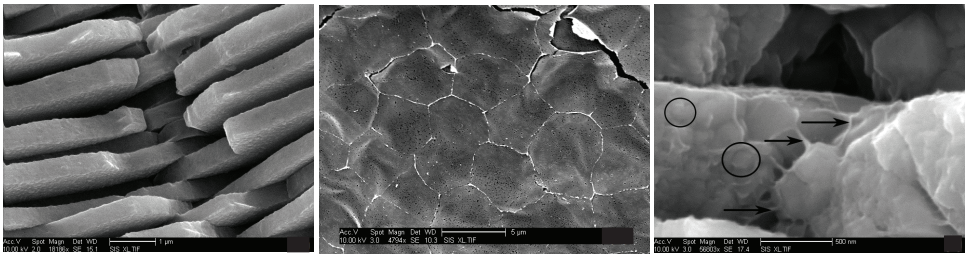

Figure 1: *SEM images showing the structure of nacre. (a) A section of fractured shell shows parallel layers of ∼500 nm thick tiles between which are sandwiched interlamellar organic layers. (b) Interlamellar layers with polygonal tile imprints remaining after demineralization of nacre with EDTA. (c) Tiles consisting of aragonitic nanograins encased in a protein matrix. Circles are placed around two individual nanograins and arrows point to the surrounding protein matrix.*

1979; Weiner and Traub, 1980; Poulicek, 1983; Weiss *et al.*, 2002) which in *H. rufescens* amounts to ∼6.4 wt% Bezares *et al.* (2008). The predominant model for il-layer structure is based on TEM observations of il-layer fragments (Watabe, 1965; Weiner, 1979; Weiner and Traub, 1980; Nakahara, 1979, 1983; Levi-Kalisman *et al.* 2001) and is depicted in (Fig. 2). It consist of an electron-lucent core of parallel β-chitin fibers sandwiched between layers of aspartic acid rich macromolecules. To date observations of chitin fiber alignment within il-layers have only been made using fragments of material and thus nothing has been said about the potential alignment of fibers across numerous il-layers or alignment with respect to the growth direction of the shell. Alignment between chitin fibers and the crystallographic axes of single tiles has been found in the nacres of numerous mollusks (Weiner and Traub, 1980; Weiner *et al.* 1983). Of significance to this study is that in the class *cephalopoda*, and more specifically in *N. rupertus* chitin fiber axes were aligned "along the direction of bilateral symmetry" of the shell, that is aligned normal to the growth direction of the shell. A similar fiber-growth direction alignment can be inferred by combining the findings by Wada (1958) that tile b-axes in the bivalve *P. martensii* are normal to the growth direction of the shell with the results by Weiner *et al.* (1983) that in the same species chitin fibers are aligned with the b-axes of tiles. Our current findings indicate that in a third class of mollusks gastropods, and more specifically in *H. rufescens*, chitin fibers are also aligned normal to the growth direction.

Moreover this alignment is found over all il-layers imaged where the native orientation of il-layers has been maintained, and across areas covering square millimeters!

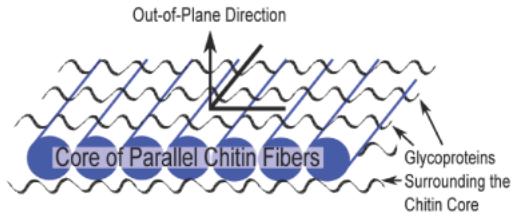

Figure 2: *Schematic diagram of the interlamellar layer structure according to Levi-Kalisman* et al. *(2001) and Bezares* et al. *(2008). Uni-axially aligned chitin fibers form a core within individual il-layers, the core is encased in layers of glycoproteins.*

The structure of il-layers, specifically, in *H. rufescens*, has been imaged *via* AFM following the degradation of matrix layers with various proteases (Schaffer *et al.*, 1997; Bezares *et al.*, 2008). Schaffer *et al.* (1997) uncovered evidence of apparently randomly oriented fibers ∼10 nm wide between which 5-50 nm diameter pores were formed. The fibers were suggested to be chitin or unidentified protein but without differentiation or verification. A model for tile nucleation and growth across il-layers was presented where the pores were sites through which growing aragonite could traverse il-layers in what were termed "mineral bridges". Using AFM imaging, coupled with various histochemical techniques and following similar proteolytic treatments of il-layers Bezares *et al.* (2008) came to the conclusion that the fibers were indeed chitin with a far more organized structure; this was later used in developing a viscoelastic constitutive model for il-layer mechanical response by Bezares *et al.* (2010). Our current findings now extend those of Bezares *et al.* (2008), but are in accordance with the conceptual model of Levi-Kalisman *et al.* (2001). We find that after both alkaline and proteolytic degradation of il-layer protein a core of aligned chitin fibers is exposed with pores being due to gaps forming between fibers which partially retain some lateral connectivity.

From a mechanical standpoint the issue of fiber orientation is of great significance in biological structures Wainwright *et al.* (1976) in particular when properties such as material stiffness and relaxation times are measured using uni-axial tensile tests. Such tests were performed by Bezares *et al.* (2010) on il-layers extracted from the nacre of *H. rufescens.* The viscoelastic

response of il-layers was characterized by fitting a linear Kelvin model to their relaxation data, which rendered parameters of $E_0 = (0.668 \pm 0.088)$ GPa, $E_1 = (0.311 \pm 0.092)$ GPa, and $\eta = \tau E_1 = (42 \pm 0.37 \times 10^6)$ Pa·s, where τ is the relaxation time constant. It was also found that chitin fibers were the major contributor to il-layer stiffness verifying the previous suggestion by Weiner *et al.* (1983) that the chitin core might serve a mechanical function as the structural framework of il-layers. The significance of the connectivity between individual chitin fibers, essential for the transfer of load across samples which included thousands of tile imprints, was briefly discussed but not investigated. Here we address the issue of fiber-fiber connectivity and its effect on the mechanical response of il-layers. Our current finding that chitin fibers are uni-axially aligned indicates that the elastic and viscoelastic properties of il-layers should be orthotropic. The alignment might also have a measurable effect on the stiffness and toughness of nacre at the macro scale due to the key role of chitin in providing il-layer stiffness and the importance of il-layers to mechanical response of nacre.

In what follows we present a series of SEM images documenting the successive removal of protein from il-layers by alkaline and proteolytic treatments which expose a structural core of uni-axially aligned chitin fibers. The growth of mineral bridges through the chitin core specifically and the porosity of il-layers are discussed in terms of these new findings. We propose that the alignment of chitin fibers normal to the shell growth direction as we present herein for the gastropod *H. rufescens* may also be found in other classes of mollusks. The implications of fiber alignment within single il-layers to the mechanical response of nacre are then discussed in terms of a more complete constitutive model for the nacre il-layers; the full description of this model is left for Part II of this series. Our hope is that this model will find applicability in fields such as soft-tissue engineering and prosthetics design where bio-mineral/bio-polymer interfaces will be of inevitable interest.

2 Materials and methods

2.1 Shell samples

Fresh shells from *H. rufescens*, raised under conditions of constant temperature and diet so as not to develop so-called "green layers", were obtained from The Abalone Farm Inc. in Cayucos, CA. and stored dry at 4 °C. Rectangular shell sections, 10 x 25 mm in size, were cut out of shells with their longer sides

normal to the growth direction, extensively washed in dI, and demineralized in 0.5 M EDTA pH 8.0 containing 0.5% Cetylpyridinum Chloride (Sigma) as an antiseptic, under gentle shaking for three weeks at 20 °C.

2.2 Alkaline peroxidation

The alkaline peroxidase solution was prepared following Moses *et al.* (2006) and consisted of 5% 10 N NaOH, 10% concentrated hydrogen peroxide, and 85% Milli-Q water. Demineralized samples were submerged for 1 h at 70 °C in this solution after which they were washed in dI.

2.3 Enzymatic digestion with proteinase-K

Following protein removal by alkaline peroxidation, samples were incubated in a solution of 5 mM Hepes buffer, pH 7.5 containing 200 μg/mL of proteinase-K (Sigma) for 3 days at 20 °C. Samples were then extensively washed in dI.

2.4 Calcofluor white staining

Two staining reagents were prepared as follows: A 10% KOH solution was prepared by dissolving 10 g of KOH in 90 mL of dI to which 10 mL of glycerin were added. A second reagent was prepared by dissolving 0.1% of fluorescent brightener 28 (Sigma) in 100 mL of dI under gentle heating. Samples were stained by adding two drops of each reagent to il-layers previously mounted on glass slides for 4 min after which samples were rinsed in dI, air dried and mounted in Entellan mounting medium (Merck).

2.5 Optical microscopy

Calcofluor White stained samples were imaged with a Nikon Eclipse 80i optical microscope using a 11003 V3 filter set (Chroma).

2.6 Scanning electron microscopy

Samples were dehydrated in an ethanol series, critical point dried, coated with Iridium and imaged with a Philips XL30 ESEM.

3 Results

The alkaline treatment of bulk demineralized bio-polymer framework material leaves completely translucent samples as shown in (Fig. 3a) where an estimated 80 wt% of dry organic material has been removed from the as-demineralized material. Epi-fluorescence imaging of translucent il-layers stained with Calcofluor White show strong fluorescence of entire sheets as in (Fig. 3b).

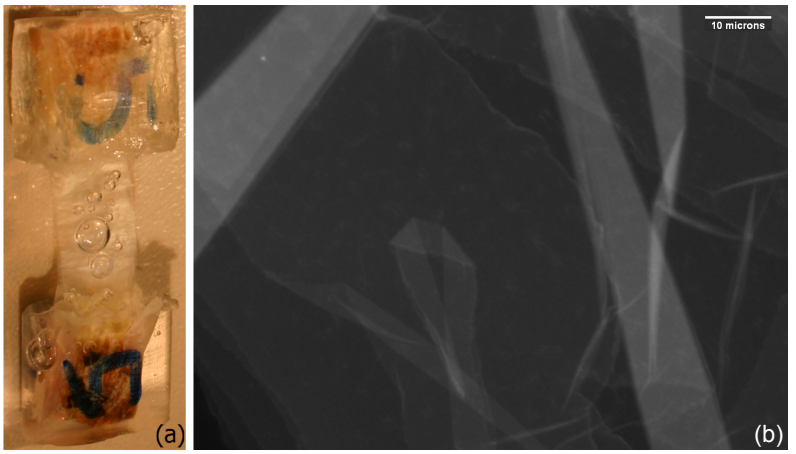

Figure 3: *(a) The translucent material remaining after alkaline peroxidation has removed ∼80 wt% of organic material. (b) Calcofluor white staining of il-layers after alkaline treatment shows that the remaining material is chitin.*

Following the partial removal of protein by alkaline treatment alone, il-layers appear perforated with holes generally appearing round with diameters in the range of 10-50 nm as shown in (Fig. 4a). The size and distribution of these holes over regions that in some cases span square millimeters for the most part are fairly uniform. In some regions of such samples the holes take on an oblong shape with their longer axes aligned as evident in (Fig. 4b). A greater degree of protein removal appears to have taken place in these regions where the holes look more like gaps between parallel fiber-like structures.

The additional removal of protein with proteinase-K reveals entire sheets of uni-axially aligned and densely packed fibers as evident in (Fig. 5a). In regions where sheets are slightly pulled apart laterally it is seen that the fiber bundles consist of ∼10 nm diameter fibers bound to each other laterally but clearly uni-axially aligned. What were previously oblong holes now are clearly

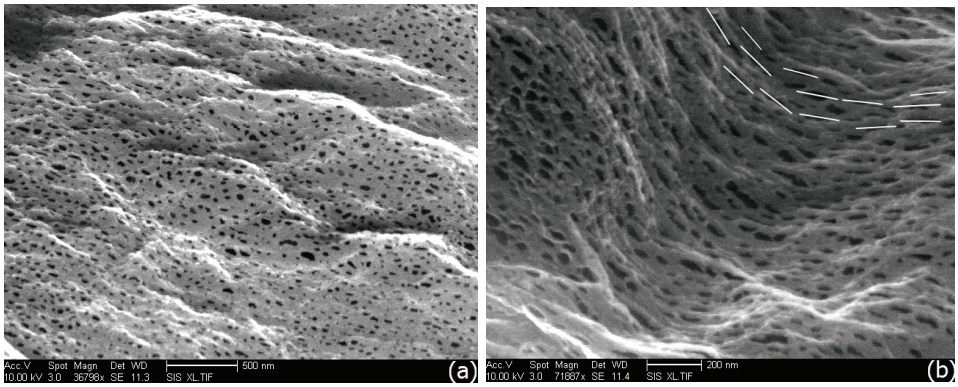

Figure 4: *SEM image of sheets having undergone alkaline treatment. (a) Round 10-50 nm diameter holes are uniformly distributed over framework layers. (b) In some regions the holes appear larger and oblong with their long axes aligned and take on the appearance of gaps between fibers. White lines at the top right of the image indicate the long axes of individual holes and are aligned over the surface of the folded il-layer.*

seen to be gaps between fibers which still maintain some lateral connectivity as seen in (Fig. 5b).

Larger, and round, rather than oblong holes consistently of ∼100 nm in diameter appear in some regions and are approximately 2-3 μm apart though it is difficult to judge their precise spacing due to the sheets being folded. Along the borders of the holes, fibers do not appear frayed but seem to form continuous rings as evident in (Fig. 6).

Images of multiple sheets from numerous il-layers show that fibers are co-aligned across multiple sheets. Having taken into consideration the direction of the samples with respect to the growth direction of the shell, as described in the materials and methods section, we find that the bundles in all layers are normal to the growth direction as noted in (Fig. 7).

4 Discussion

4.1 Identification of a chitin core within interlamellar layers

It has been estimated that approximately 75-80 wt% of the insoluble organic matrix comprising il-layers consists of acidic glycoproteins Addadi and Weiner, (1985). Alkaline peroxidase treatment of il-layers removes ∼80 wt%

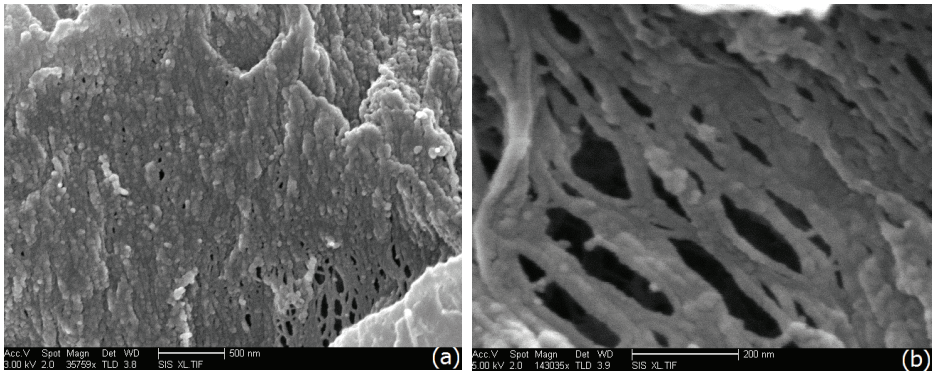

Figure 5: *SEM image of il-layers after alkaline and proteolytic treatments. (a) The sheets can appear to consist of densely packed uni-axially aligned fiber bundles. (b) Where sheets have been pulled apart laterally it becomes clear that they consist of uni-axially aligned and laterally bound single fibers.*

of organic material and leaves behind il-layers which strongly fluoresce under Calcofluor White staining. Calcofluor White preferentially labels β-1-4 polysaccharides such as chitin indicating that the remaining material is in fact chitin in particular considering the amount of protein removed. The translucent appearance of alkaline treated samples (see Fig. 3a) is quite similar to that of the chitin framework exposed in jumbo squid beaks having undergone the same alkaline peroxidase treatment Miserez *et al.* (2008). To clearly expose individual chitin fibers, as seen in (Fig. 5b), requires the successive alkaline and enzymatic degradation of protein in il-layers. Individual fibers are not as clearly visible in samples having undergone alkaline treatment alone (Fig. 4a). It has previously been noted that even after alkaline hydrolysis of il-layers, protein remains bound to chitin Zents *et al.* (2001) which may explain why the additional proteinase-K treatment was necessary in this study to clearly expose individual fibers as shown in (Fig. 5).

4.2 Porous structure of interlamellar layers

Previous AFM images of il-layers extracted from *H. rufescens* nacre by demineralization and proteolitically treated show a porous appearance where pores are approximately round and with diameters of $\sim$50 nm (Schaffer *et al.*, 1997; Bezares *et al.*, 2008); these AFM images however span only a few microns. SEM imaging of alkaline peroxidase treated il-layers provide much

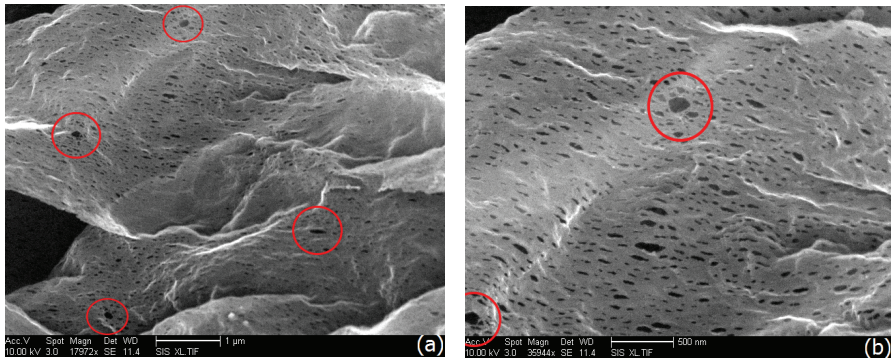

Figure 6: *SEM image showing (a) ∼100 nm diameter round holes in il-layers having undergone alkaline treatment alone which are spaced ∼2-3 µm apart. (b) A close up of these larger holes shows that their edges are not frayed or oblong but instead form closed rings.*

sharper images, making clear the size and distribution of pores which are 10-50 nm wide, in agreement with the findings of the aforementioned AFM studies (see also Fig. 4a). With the further removal of protein by proteinase-K treatment ∼10 nm diameter chitin fibers are exposed which are connected laterally at points ∼200 nm apart (Fig. 5b). What previously appeared to be pores are in fact aligned gaps between these fibers and are no longer round but oblong in shape with shorter and longer axes having lengths of approximately 10 nm and 200 nm, respectively. That in some cases, such as in (Fig. 5a), the fibers are densely packed together, hiding the pores, may be an artifact of the drying process during which pores may have collapsed due to capillary forces. The randomly orientated fibers previously imaged *via* AFM are now entirely gone with the complete removal of protein Bezares *et al.* (2008), indicating that the fibers in those studies were in fact protein and not chitin.

4.3 Mineral bridges and major connections

Tile surfaces are covered with nodules (Fig. 8a) which have been called "mineral bridges" as it was proposed that they formed continuous mineral connections between tiles across il-layers Schaffer *et al.* (1997). Mineral bridges have an approximate size of 10-50 nm and are longer along one direction than the other as in (Fig. 8a), where the insert shows that their lengths also have a certain amount of alignment similar to what is found in il-layer

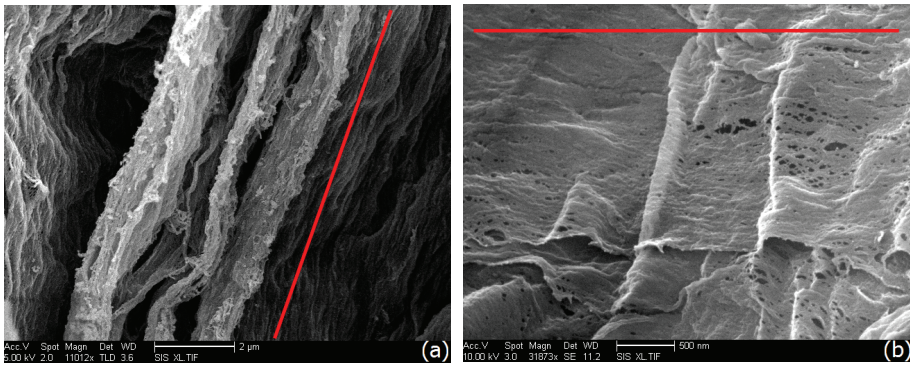

Figure 7: *SEM images of il-layers having undergone both alkaline and enzymatic treatments. (a) Fibers in four consecutive il-layers are lined up in parallel. The red line in the il-layer plane is normal to the shell's growth direction. (b) Three chitin core sheets lie on top of each other with their respective fibers aligned. The red line in the il-layer plane is normal to the shell's growth direction.*

pores (Fig. 4b). Recent SEM imaging of nacent tiles growing in gastropod nacre has revealed that mineral bridges result from mineral growing into il-layer pores but not fully traversing them to form continuous connections, see Fig. 6 in Checa *et al.* (2011). Tiles do have a central protein rich region which can be exposed by alkaline treatment (Fig. 8b). These regions are the nucleation points on pre-existing tiles where the mineral for a new growing tile first traverses the il-layer above it, upon which the new tile grows (Fig. 9a). The protein rich regions have a diameter of ∼100 nm. To differentiate between true tile-tile connections and mineral bridges true connections have now been called major connections Checa *et al.* (2011). A comparison between the number and size of il-layer pores i.e. 10-50 nm as in (Fig. 4a) and the number and size of mineral bridges on tiles (Fig. 8a) shows that they are similar in size and distribution, supporting the finding that pores serve as locations into which mineral grows during tile formation Checa *et al.* (2011). The larger holes in (Fig. 6), with ∼100 nm diameters and spaced at least 2-3 μm apart closely match those of major connections. These holes are most likely the points of traversal of growing tiles through the il-layer chitin core.

The surface texture of tiles may alternatively be interpreted as being the remaining imprints of il-layers after they have been removed as in (Fig. 8) where an alkaline treatment was used. A schematic drawing of the resulting surface texture is shown in (Fig. 9b). Tile surface texture reveals that within

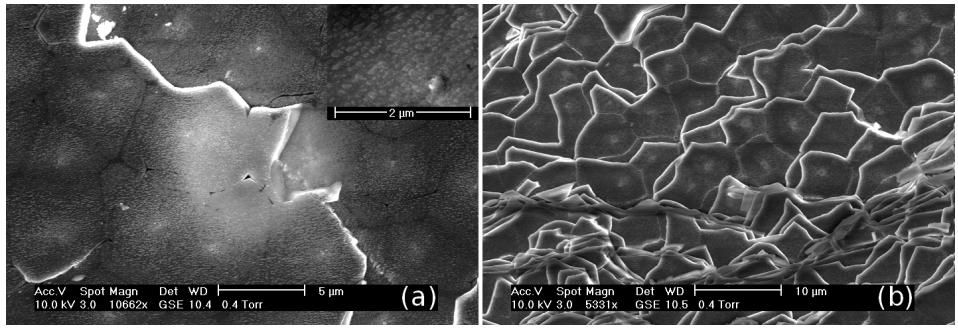

Figure 8: *SEM images of cleaved nacre having undergone a light alkaline treatment to remove surface protein. (a) Tile surfaces are covered with ∼10-50 nm diameter "mineral bridges" as described by Schaffer* et al. *(1997) which are not circular but are longer along one direction. The insert shows that the mineral bridges are aligned along the direction of their lengths. (b) The lighter regions at the center of tiles with diameters of ∼100 nm are the locations of the "major connections" described by Checa* et al. *(2011).*

intact nacre fibers are not pressed together in sheets as in (Fig. 5a) but are in fact configured with gaps and the fiber-connectivity that leaves pores with dimensions and arrangement close to what is seen in (Fig. 4b).

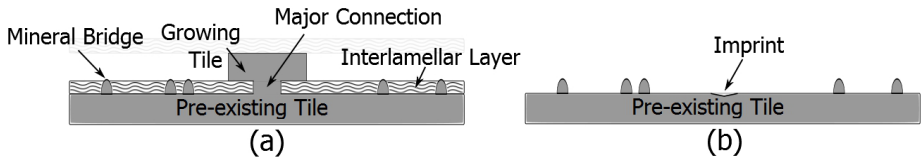

Figure 9: *A schematic drawing of the tile nucleation and growth process showing the differences between mineral bridges and major connections, and the remaining surface texture following il-layer removal. a) The smaller mineral bridges (∼10-50 nm wide) grow into il-layer pores also (∼10-50 nm wide) but do not form continuous links between tiles. On the other hand major connections (∼100 nm wide) completely traverse il-layers forming wide continuous mineral connections between tiles. b) Tile surface texture remains after tile lamellae have been cleaved apart and il-layers removed; the imprint at the center of the tile marks the previous location of a major connection.*

Organic framework tissue can deform substantially after being extracted by demineralization as for example in (Fig. 5a) where fibers are closely packed in one region and spread apart in another. Deforming il-layers extracted from

demineralized nacre would likely result in layer 'damage' in the form of pore coalescence or fiber breakage. An analysis of extracted il-layers undergoing significant deformation would require some consideration of these kinds of effects. Within intact nacre however il-layers are completely confined by surrounding mineral. From il-layer imprints on tiles such as in (Fig. 5 and Fig. 7b) an estimation of fiber orientation within intact nacre can be made. Measuring the angle ϕ as shown in (Fig. 10), between lines diagonally across the points of lateral connection between fibers results in $\phi = 30 \pm 5°$.

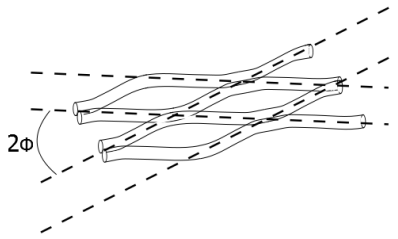

Figure 10: *A drawing describing the angle formed by lines drawn diagonally across the points of connection between chitin fibers. From images such as (Figs. 5 and 7b) the angle ϕ is estimated to be $30 \pm 5°$.*

4.4 Chitin fiber orientation with respect to the direction of shell growth

In the nacre of two classes of mollusks, bivalves and cephalopods, chitin fiber b-axes have been found to lie normal to the growth direction of the shell within il-layers (Wada, 1958; Weiner *et al.* 1983). X-ray and electron diffraction techniques were used in those studies, which involved imaging small fragments of il-layers extracted from pieces of shell. As such, the alignment of chitin fibers with respect to the direction of shell growth, and the alignment of fibers in multiple consecutive il-layers, could not have been investigated. These two limitations would have been encountered in the Cryo-TEM work of Levi-Kalisman *et al.* (2001), as well, since il-layer fragment suspensions were used in that study. In the present study, SEM imaging following alkaline and proteolytic treatments has permitted chitin fiber alignment to be studied over large areas compared to previous XRD, ED, and TEM studies. Furthermore the orientation of individual il-layers is maintained (Fig. 7) which is not possible when using il-layer sections or fragment suspensions because layers lose their initial and relative orientations. Beginning with large

samples of demineralized nacre, where the growth direction of the shell was first noted, we find that chitin fiber alignment in all layers is normal to the direction of shell growth, adding now gastropods to the classes of mollusks where chitin fibers are aligned in this manner. Considering the manner of shell growth in all classes of mollusks whereby tiles are added at the edge of the shell in rows parallel to the edge (i.e. normal to the direction of shell growth), it would seem natural for the chitin core to also grow at the shell edge by the addition of fibers in the same parallel manner. We suspect that the alignment of fibers normal to the direction of shell growth observed in this study for the gastropod *H. rufescens* is to be found in most if not all classes of mollusks. A summary of our current observations of chitin fiber alignment within single il-layers is presented in (Fig. 11) below, where they are compared and contrasted to previous chitin core structural models.

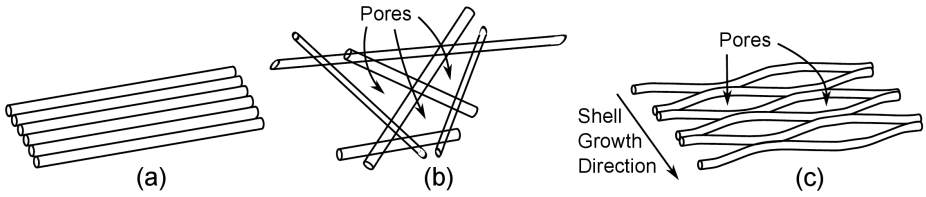

Figure 11: *A schematic drawing of chitin fiber alignment within an interlamellar layer according to two previously proposed models and the current observations. (a) Fibers are uni-axially aligned and no pores are located between them Levi* et al. *(2001). (b) Fibers are randomly oriented with the spaces between fibers taking on the form of pores Bezares* et al. *(2010). (c) Based on our current findings chitin fibers are uni-axially aligned, pores are formed by the gaps between fibers that are laterally connected only at certain points, and all fibers are oriented normal to the growth direction of the shell.*

4.5 Implications for mechanical response

Considering that chitin fibers are oriented normal to the direction of shell growth, and in view of the finding by Bezares *et al.* (2010) that chitin is the principle contributor to the stiffness of il-layers, it is to be expected that the organic framework has a greater tensile stiffness in the direction normal to that of shell growth. In Bezares *et al.* (2010) the structural integrity of il-layers was entirely lost following the degradation of chitin with chitinase where only protein remained, while the stiffness was hardly affected by the enzymatic removal of most but not all protein. In an il-layer under uni-axial

tension with the loading direction being normal to the fiber direction, the protein matrix but not the fibers would be loaded; this is akin to testing an il-layer where chitin has been removed but protein remains. This suggests that the stiffness of il-layers tested in tension in a direction transverse to the chitin fiber direction should be vanishingly small due to the low stiffness of protein alone.

Being that single tiles in brick-wall-like tile lamellae do not have a preferred orientation and that individual tiles behave as isotropic solids, Bezares *et al.* (2011) suggested that tile lamellae and thus nacre could be considered as transversely-isotropic. Interlamellar layers which we have shown to be orthotropic, with chitin fibers uni-axially aligned, make nacre a layered composite of alternating isotropic and orthotropic lamina, in which all orthotropic layers (il-layers) are co-aligned. As such nacre as a whole might exhibit an orthotropic response. For example, a mode-I type crack propagating along the growth direction of the shell, in a plane normal to il-layers, should place chitin fibers in tension, while a mode-I crack running normal to the growth direction and normal to il-layers should split the chitin fibers. The contribution of chitin fiber alignment to this kind of response has yet to be quantified.

4.6 Framework for a viscoelastic model for a bio-polymer interlamellar layer

Based on the initial findings of Bezares *et al.* (2010), and on the novel findings reported on herein, we propose models for the bio-polymer il-layers as sketched in (Figs. 12a,b). Figure 12a implies that the structural chitin

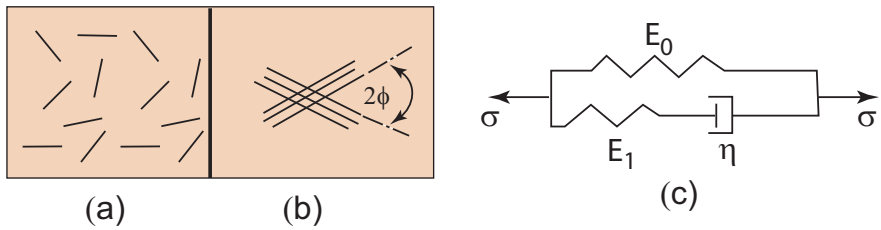

Figure 12: *Models (a) and (b) representing either transversely isotropic (randomly oriented fibers) or orthotropic (aligned sets of fibers) structures, respectively. (c) A Kelvin viscoelastic model used by Bezares* et al. *(2010) fitted to their data on mechanical testing of il-layers.*

fiber network is composed of, essentially, in-plane extended and connected, randomly oriented, fibers. Note that the fibers should be seen as extended whereas the figure indicates only their orientation; this was the scenario envisioned by Bezares *et al.* (2010) and used in their analysis. Figure 12b, on the other hand, depicts long extended fibers, but with aligned orientation. This is orthotropic in the plane as discussed above. If the fibers are aligned, the angle ϕ would be small, with $\phi \to 0$ if the fibers are perfectly aligned. In Part II of this series we develop detailed viscoelastic constitutive models for both structural motifs.

The material constitutive response has been confirmed by Bezares *et al.* (2010) to be viscoelastic. To be specific they successfully fit a linear Kelvin model shown in (Fig. 12c) to their relaxation data, finding that $E_0 = (0.668 \pm 0.088)$ GPa, $E_1 = (0.311 \pm 0.092)$ GPa, and $\eta = \tau E_1 = (42 \pm 0.37 \times 10^6)$ Pa·s, where τ is the relaxation time constant. Indeed, an entirely acceptable fit would have been found with even simpler linear models. This can be accomplished, for example, by setting $E_1 \to \infty$, i.e., removing elastic element E_1 from the model, with suitable adjustment of E_0, as noted by Bezares *et al.* (2010).

5 Conclusions

For the first time to our knowledge we have provided direct evidence *via* SEM imaging that a core of chitin fibers exists within il-layers of gastropod nacre arranged in parallel not only within individual layers but in all layers and, quite surprisingly, normal to the growth direction of the shell. The parallel arrangement within single il-layers fully supports the currently accepted il-layer structure model suggested by Levi-Kalisman *et al.* (2001). Exposing the chitin core requires protein removal by consecutive alkaline and enzymatic treatments. Closed circular holes with diameters of $\sim$100 nm are frequently found with a center to center spacing that suggests that these may be the locations where major connections (i.e., mineral bridges) traverse single il-layers by spreading apart rather than tearing individual fibers. Our findings of fiber alignment have a number of important implications to the mechanical properties of nacre as we hypothesize that the stiffness of single il-layers should be orthotropic, with the stiffness transverse to the fiber orientation being vanishingly small in comparison to that along the fiber length. To ascertain this would require performing a comprehensive investigation as outlined in Bezares *et al.* (2010), where samples would be tested in tension

along the direction of shell growth; this could be achieved using a more sensitive experimental approach such as is described in Opdahl and Somorjai (2001) for PDMS films. Such experiments would be required for the calibration of an anisotropic viscoelastic model for nacre, but this is beyond the present scope and is left for future investigation. Our findings of chitin fiber alignment in relation to growth direction for gastropod nacre are consistent with previous similar findings for bivalve and cephalopod nacres, which suggests that this may be the case for other classes of mollusks. This should be investigated by a comparative study using the alkaline and proteolytic treatments described herein, which would require the SEM imaging of chitin fiber orientation over large length scales. Successful modelling remains an open area of investigation of great importance for bio-duplication and novel material development.

Acknowledgements

The authors would like to thank the reviewers provided by this journal for their comments and recommendations which have greatly improved the quality of this paper. We also extend our thanks to Ryan Anderson at the Nano3 facility at UCSD for his assistance with the SEM imaging.

References

[1] Addadi, L., Weiner, S., 1985. Interactions between acidic proteins and crystals: stereochemical requirements in biomineralization. Proc. Natl. Acad. Sci. USA 82, 4110–4114.

[2] Baeuerlein, E., 2000. Biomineralization: From Biology to Biotechnology and Medical Application. Wiley-VCH, New York.

[3] Bezares, J., Asaro, R.J., Hawley, M., 2008. Macromolecular structure of the organic framework of nacre in Haliotis rufescens: implications for growth and mechanical behavior. J. Struct. Biol. 163, 61–75.

[4] Bezares, J., Asaro, R.J., Hawley, M., 2010. Macromolecular structure of the organic framework of nacre in Haliotis rufescens: implications for mechanical response. J. Struct. Biol. 170, 484–500.

[5] Bezares, J., Peng, Z.L., Asaro, R.J., Zhu, Q., 2011. Macromolecular structure and viscoelastic response of the organic framework of nacre in Haliotis rufescens: a perspective and overview. Theoret. Appl. Mech. 38, 75–106.

[6] Cariolou, M.A., Morse, D.E., 1988. Purification and characterization of calcium binding conchiolin shell peptides from the mollusk, Haliotis rufescens, as a function of development. J. Comp. Physiol. B 157, 717–729.

[7] Checa, A.G., Cartwright, J.H.E., Willinger, M.G., 2011. Mineral bridges in nacre. J. Struct. Biol. 176, 330–339.

[8] Crenshaw, M.A., 1972. The soluble matrix of Mercenaria mercenaria shell. Biomineral Res. Rep. 6, 6–11.

[9] Currey, J.D., 1977. Mechanical properties of mother of pearl in tension. Proc. R. Soc. Lond. B 196, 443–463.

[10] Evans, A.G., Suo, Z.,Wang, R.Z., Aksay, I.A., He, M.Y., Hutchinson, J.W., 2001. Model for the robust mechanical behavior of nacre. J. Mater. Res. 16, 2475–2484.

[11] Gao, H., Ji., Jager, I.L., Arzt, E., Fratzl, P. 2003. Materials become insensitive to flaws at nanoscale: lessons from Nature. PNAS 100, 5597–5600.

[12] Goffinet, G., Jeuniaux, C., 1979. Distribution et importance quantitative de la chitine dans les coquilles de mollusques. Cah. Biol. Mar. 20, 341–349.

[13] Gregoire, C., 1957. Topography of the organic components in mother-of-pearl. J. Biophys. Biochem. Cytol. 3, 797–808.

[14] Gregoire, C., 1972. Structure of the molluscan shell. In: Florkin, M., Scheer, B.T. (Eds.), Chemical Zoology. Academic Press, New York, pp. 45–102.

[15] Jackson, A.P., Vincent, J.F.V., Turner, R.M., 1988. The Mechanical Design of Nacre. Proc. R. Soc. Lond. B 234, 415–440.

[16] Levi-Kalisman, Y., Falini, G., Addadi, L., Weiner, S., 2001. Structure of the nacreous organic matrix of a Bivalve Mollusk shell examined in the hydrated state using cryo-TEM. J. Struct. Biol. 135, 8–17.

[17] Lowenstam, H.A., Weiner, S., 1989. On Biomineralization. Oxford University Press, New York.

[18] Miserez, A., Schneberk, T., Sun, C., Zok, F.W., Waite, J.H., 2008. The Transition from Stiff to Compliant Materials in Squid Beaks. Science 319, 1816–1819.

[19] Moses, D.N., Harreld, J.H., Stucky, G.D., Herbert Waite, J., 2006. Melanin and Glycera Jaws. Emerging dark side of a robust biocomposite structure. J. Biol. Chem. 281, 34826–34832.

[20] Nakahara H., 1979. An electron microscope study of the growing surface of nacre in two gastropod species, Turbo cornutus and Tegula pfeifferi. Jpn. J. Malacol. 38, 205–211.

[21] Nakahara, H., 1983. Calcification of gastropod nacre. In: Westbroek, P., de Jong, E.W. (Eds.), Biomineralization and Biological Metal Accumulation. Dordrecht: Reidel, pp. 225–230.

[22] Nudelman, F., Gotliv, B.A., Addadi, L., Weiner, S., 2006. Mollusk shell formation: mapping the distribution of organic matrix components underlying a single aragonitic tablet in nacre. J. Struct. Biol. 153, 176–187.

[23] Opdahl, A., Somorjai, G.A., 2001. Stretched polymer surfaces: atomic force microscopy measurement of the surface deformation and surface elastic properties of stretched polythylene. J. Polymer Sci B-Polymer Phys 39, 2263–2274.

[24] Peters, W., 1972. Occurrence of chitin in Mollusca. Comp. Biochem. Physiol. B 41, 541–550.

[25] Poulicek, M., 1983. Chitin in Gastropod Operculi. Biochem. Syst. Ecol. 11, 47–54.

[26] Ritchie, R.O., 2011. The conflicts between strength and toughness. Nature Materials 10, 817822.

[27] Rousseau, M., Lopez, E., Stempfle, P., Brendle, M., Franke, L., Guette, A., Naslain, R., Bourrat, X., 2005. Multiscale structure of sheet nacre. Biomaterials 26, 6254–6262.

[28] Sarikaya, M., J. Liu and I.A. Aksay 1992. Nacre of abalone shell: a multifunctional nanolaminated ceramic-polymer composite material. In: Case, S. (Ed.), Results and Problems in Cell Differentiation in Biopolymers. Springer-Verlag, Amsterdam, pp. 1–25.

[29] Schaffer, T.E., Ionescu-Zanetti, C., Proksch, R., Fritz, M., Walters, D.A., Almqvist, N., Zaremba, C.M., Belcher, A.M., Smith, B.L., Stucky, G.D., Morse, D.E., Hansma, P.K., 1997. Does abalone nacre form by heteroepitaxial nucleation of by growth through mineral bridges? Chem. Mater. 9, 1731–1740.

[30] Srinivasan, P.S., 1941. The elastic properties of molluscan shells. Q.J. Indian Inst. 4, 189–221.

[31] Wada, K., 1958. The crystalline structure on the nacre of pearl oyster shell. J. Soc. Sci. Fish 24, 422–427.

[32] Wang, R.Z., Suo, Z., Evans, A.G., Yao, N., Aksay, I.A., 2001. Deformation mechanisms in nacre. J. Mater. Res. 16, 2485–2493.

[33] Wainwright, S.A., Biggs, W.D., Currey, J.D., Gosline, J.M., 1976. Mechanical Design in Organisms, Wiley, New York.

[34] Watabe, N., 1965. Studies on Shell Formation. Crystal-matrix relationships in the inner layers of mollusk shells. J. Utrastruct. Res. 12, 351–370.

[35] Weiner, S., 1979. Aspartic acid-rich proteins: major components of the soluble organic matrix of mollusk shells. Calcif. Tissue Int. 29, 163–167.

[36] Weiner, S., Traub, W., 1980. X-ray diffraction study of the insoluble organic matrix of mollusk shells. FEBS Letters 111, 311–316.

[37] Weiner, S., Traub, W., 1983. Electron diffraction of mollusk shell organic matrices and their relationship to the mineral phase. Int. J. Biol. Macromol. 25, 325–328.

[38] Weiss, I.M., Renner, C., Strigl, M.G., Fritz, M., 2002. A simple and reliable method for the determination and localization of chitin in abalone nacre. Chem. Mater. 14, 3252–3259.

[39] Zents, F., Bedouet, L., Alameida, M.J., Milet, C., Lopez, E., Giraud, M., 2001. Characterization and quantification of chitosan extracted from nacre of the abalone Haliotis tuberculata and the oyster Pinctada maxima. Mar. Biotechnol. 3, 36–44.

Submitted in September 2012., revised in October 2012.

Struktura hitinskih vlakana u interlamelama sedefa *Haliotis rufescens*. Deo I: Uticaji na rast i mehanička svojstva

Koristeći seriju alkaličnih i proteolitičnih tretmana interlamelarnog sloja sedefa *Haliotis rufescens*, izdvojena je srž paralelnih hitinskih vlakana. Na bazi SEM utvrdjeno je da su hitinska vlakna ortogonalna na pravac rasta ljuske. Mineralni mostovi se fomiraju izmedju vlakana na odredjenim mjestima strukture, što doprinosi anizotropnim mehaničkim svojstvima i krotosti strukture. Konstitutivna analiza anizotropnog viskoelastičnog ponašanja *Haliotis rufescens* ljuske je diskutovana. Detaljnija analiza je predmet drugog dela ovog rada.

doi:10.2298/TAM1203209M Math. Subj. Class.: 74L15; 74C10; 74A40; 82D80.